Article

Not peer-reviewed version

Multi-Objective Optimisation Design of Urban Morphology Driven by Climate Adaptation

Shiwen Zhou , Yafei Yue , Sui Li * , Jiayi Sun

Posted Date: 7 April 2026

doi: 10.20944/preprints202604.0445.v1

Keywords: urban climate elements; urban morphology; multi-objective optimisation; spatial regression

Article

Multi-Objective Optimisation Design of Urban Morphology Driven by Climate Adaptation

Shiwen Zhou [1], Yafei Yue [1], Sui Li [2,*] and Jiayi Sun [1]

[1] School of Architecture and Planning, Shenyang Jianzhu University, Shenyang, Liaoning 110168, China
[2] JangHo Architecture College, Northeastern University, Shenyang, Liaoning 110169, China
* Correspondence: lisui0517@126.com

Abstract

Urban morphology significantly influences climate processes, and multiple climate elements respond to and provide feedback on urban morphology. In this study, we propose a methodology for monitoring and quantifying the indicators of urban climate elements. Considering the Tiexi District of Shenyang City as the study area, we explore the correlation between urban morphology and various climate elements, screen common indicators of urban morphology parameters as variables and establishe a multiple regression model for urban morphology and climate elements. The results show that the multiple regression model has a good explanation ability for the indicators of climate elements, and the building density, normalised difference vegetation index, impervious surface fraction and sky view factor are the common indicators of the microclimate elements. The road network density and sky view factor are the common indicators of atmospheric environment elements. Further, a mathematical method of multi-objective optimisation is used to integrate the regression functions of various climate-element indicators to obtain a Pareto-optimal urban morphology. Ultimately, the optimised surface temperature, surface humidity, CO2 pollution and PM2.5 pollution magnitudes are determined to be 5.84%, 18.95%, 42.65% and 13.68%, respectively. Thus, we explore a synergistic optimisation method for multiple climate elements considering spatial planning.

Keywords: urban climate elements; urban morphology; multi-objective optimisation; spatial regression

1. Introduction

Extreme weather events such as heat waves, torrential rains and floods and atmospheric pollution have posed severe challenges to the sustainable development of human society, and the impacts of climate change will be long-lasting and irreversible. The Intergovernmental Panel on Climate Change has highlighted that the decelopment of climate-adapted cities will be vital means of coping with climate change for mankind for a certain period of time in the future. Most countries have stipulated action plans for 2030, in which strengthening research on the structure and processes of urban ecosystems and multi-scale climate elements, improving the structure and processes of urban ecosystems, mitigating negative climate elements elicited by urbanisation through the control of human activities and optimising the urban morphology and spatial patterns have been focused for the sustainable development of cities.

Urban ecological processes involve energy transmission and material cycling within and between certain urban ecosystems (Inostroza & Zepp, 2021; Inostroza, 2018; Krueger et al., 2022). The pattern-process theory of landscape ecology has provided strong support for the optimisation of ecological effects at the level of spatial patterns. In built-up areas of cities, the landscape pattern manifests as a three-dimensional (3D) morphology comprising buildings and sub-surfaces, resulting from the emergence, growth, morphology, structure, function and development of human agglomerations(Fu et al., 2006). Changes in the urban sub-surface nature cause changes in the urban

 doi:10.20944/preprints202604.0445.v1

surface energy balance, considerably affecting the momentum, heat and material exchange processes of the atmosphere, thus generating a morphology of special localised climate elements within the city. Moreover, the climate elements generate a series of responses to the urban morphology through feedback generated by human activities (Ferguson& Woodbury, 2007; Taniguchi et al., 2008; Tsirigoti & Tsikaloudaki, 2018). Currently, the multi-factor coupling characteristics and spatial responses of urban morphology have become research hotspots in the field of planning (Ke et al., 2021; Yang et al., 2022; Shi et al., 2022; Gao et al., 2022). Admittedly, there are several bottlenecks in climate adaptation mechanisms for urban morphology. (1) The response mechanism of local climate to the urban morphology with multi-factor coupling has to be further clarified. Local climate elements are influenced by several urban factors. Although more studies have been conducted to explore the influencing elements of wind, heat and other climatic elements, the decoupling analysis methods for multi-effect local climate and multi-factor correlation mechanisms are still not developed. (2) There is a lack of a systematic approach for the synergistic optimisation of urban morphology that weighs the effects of multiple climatic environments. Currently, there are several local climate optimisation methods that are more directly related to the wind-heat environment, the atmosphere and ventilation; however, there is a lack of a comprehensive prediction and assessment method of the changes in other accompanying local climate elements. Hence, it is difficult to develop quantitative control methods for the goal-oriented synergistic optimisation of the urban morphology for diverse climatic environments. (3) In addition, there is a lack of application tools from basic research results to the whole process of optimisation design. To assess urban climate environments, there is an urgent need to establish a set of systematic climate-adaptive optimisation tools to guide the mode of urban development and construction through scientific quantitative analysis.

2. Linkages Between Urban Morphology and Urban Climate Elements

Urban morphology influences and modifies diverse climate elements. Since the 1860s, there has been a widespread concern regarding urbanisation leading to frequent ecological problems. Climate elements refer to changes in the structure and function of ecosystems caused by natural processes or human production and living activities. They specifically refer to the conditions and effects of the natural environment on which human beings depend for their survival and include micro-climate atmospheric environmental and hydrological elements. (Guenette et al., 2014; HE et al., 2019; Christensen et al., 1996). The impacts of these elements can be positive (contributing to ecological security) or negative (leading to ecological risks); therefore, climate elements can be used for integrated and holistic assessment of ecosystem stability(Schmitz et al., 2003; Grimm et al., 2016). Evaluating the ecological quality of cities through various monitoring indicators of climate elements has become a conventional method for studying the health and sustainability of urban ecosystems. With the development of urban 3D spatial morphology and multi-source ecological environmental data technology, the method of interpreting and predicting certain ecological environmental elements through urban morphological parameters has matured. In addition, the acquisition of climate-element indicators is mostly based on remote sensing, field monitoring and permorphologyance-based simulation. To reveal the correlation mechanism between urban morphology and climate elements, traditional research mostly adopts different morphologys of mathematical regression models to reveal the influence law between the two. The current development of artificial intelligence algorithms, such as deep learning and image recognition algorithms, provides the possibility of revealing the complex correlation between various climate elements and urban morphology response(Luccioni et al., 2021; Mohamed & Zahidi, 2024; Zhao et al., 2024).

2.1. Urban Morphology and Microclimate Elements

Urban micro-climate refers to the climatic conditions of a local space, specifically including air temperature, humidity and wind speed. The climatic characteristics of urban areas differ significantly from those of natural environment due to the influence of artificial environments.The influence of urban morphology on climate elements is manifested in several ways: 1) the large number of buildings and impermeable surfaces with high absorption and storage of thermal radiation, 2) the influence of undercushion roughness on flow wind and 3) the permeability and evaporative heat dissipation of surfaces with different levels of vegetation cover, resulting in significant spatial heterogeneity of local micro-climatic elements in urban areas (Jiang, 2019; Othman, 2020; Oke & Canada, 2004; Shao, 2023). Research on the correlation between urban morphology and micro-climate elements has made great progress in recent years, with building indices, spatial features, green spaces and water bodies as the main urban morphology parameters. Considering the heat island effect as an example, Jurgen P. Kropp and Deigo Rybski et al. developed a linear relationship between the intensity of the urban heat island (UHI) in a single-centre city and the logarithmic city area and logarithmic total building volume by means of urban climate simulation and then constructed a regression model for the UHI intensity, the total building volume of the city, the city size and the urban morphology (Li et al., 2020). Yang F et al.selected nine building 3D morphological indices, such as floor area ratio, average BH and buiding spatial compactness, and quantitatively analysed the correlation between building 3D spatial patterns and UHI effect of 30 provincial capitals in China using a geographically weighted regression (GWR) model (Feng et al., 2016). In terms of ventilation effects, Kubota et al. developed a mathematical model for the relationship between the mean wind speed ratio and BD and building wind angle using multiple linear regression, and performeded an ANOVA to test the quality of the regression model's quality. (Kubota et al., 2008). Shara-Eldin used multiple linear regression to develop a parametric model of the relationship between the wind pressure difference coefficient a target building and the surrounding building layout (Sharag-eldin, 2007). Zhang Shuo et al. fitted a ventilation potential index based on sky openness and aerodynamic roughness to assess the ventilation capacity of an urban surface and explored a synergistic optimisation method of wind-heat environments for urban spaces in a specific study area (Zhang et al., 2008).

2.2. Urban Morphology and Atmospheric Elements

In recent years, the issue of global greenhouse gases and atmospheric pollution has received considerable attention. Atmospheric environmental elements refer to the process of excessive emissions of greenhouse gases or pollution of the atmospheric environment caused by human activities, which change in the structure and function of the atmospheric environment (Zhou et al., 2008). Existing atmospheric environmental studies mainly focused on the influence of air pollution and carbon emissions. The influence of urban morphology on the atmospheric environmental elements is mainly reflected in the type of high-emission land use, the spatial pattern affecting pollution diffusion and the structure and quantity of green space, water bodies and other environmental indicators that reduce air pollution(Chokhachian et al., 2020). The indicators of atmospheric environmental elements are based on various methods, such as urban flux observation, remote sensing inversion and digital simulation, and the study scale ranges from macro-municipal, meso-regional to micro-site. Clark et al. studied the relationship between morphology and air pollutant concentrations in 114 U. S. cities reported that several morphology metrics, such as BD and building population centripetalism, were significantly correlated with $PM_{2.5}$ concentrations (Clark et al., 2011). Ishii et al. summarised urban morphology effects on building energy consumption in Japan and showed that a medium-density, evenly distributed urban morphology is more conducive to energy conservation and greenhouse gas emission reduction (Ishii et al., 2010). Long Ying et al., proposed a multi-intelligence body model that the energy consumption of commuter transport corresponding to various urban morphologies basically satisfies the characteristics of linear distribution(Long et al., 2011). Xiang et al. used GWR to study the relationship between green space landscape patterns and aerosols and proposed strategies for mitigating aerosol pollution targeting core landscape indices (Xiang et al., 2022). The above studies provide a good basis for the optimization of atmospheric elements from the urban morphology approach.

 doi:10.20944/preprints202604.0445.v1

The above relevant studies have laid the necessary theoretical basis for constructing of the planning framework of this study: (1) urban morphology can considerably influence and change the local climate, and there is a correlation between urban morphology and urban climate elements; (2) from the results of existing research, it can be seen that there is a clear intersection of morphological parameters that influence different climatic elements, such as micro-climate and atmosphere, including the morphological parameters of buildings, sub-surface, green spaces, and water bodies; (3) through the establishment of mathematical models, such as linear and spatial regression medels, and artificial intelligence methods, such as deep learning, it is possible to explain the influence mechanism of morphological parameters on climate elements. In this study, we quantify the correlation between spatial morphology and various climate elements from the mutual feedback principle of 'urban morphology-climate elements', construct a multi-objective optimisation model of climate elements based on urban morphology parameters and explore the response framework of spatial planning from the perspective of urban ecological synergistic optimisation.

3. Multi-Objective Optimal Planning Framework for Urban Climate Elements

This study mainly comprises three aspects: 1) the quantification of urban climate-element indicators, 2) the modelling of correlation between climate elements and urban morphology and 3) the multi-objective optimisation and regulation of urban morphology. The technical route is shown in Figure 1.

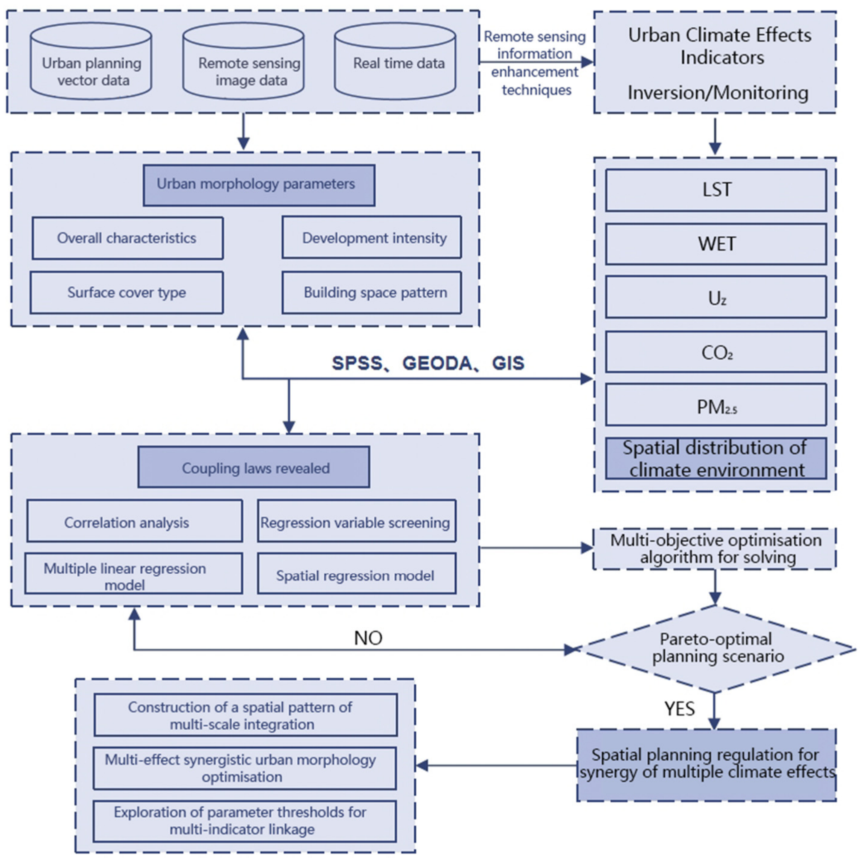

Figure 1. Planning framework technical routes.

3.1. Monitoring and Quantification of Indicators of Urban Climate Elements

The current development of remote-sensing-enhanced big data technology and the integration of heterogeneous urban ecological environment data from multiple sources provide technical support for dynamic monitoring of the urban ecological environment quality and accurate detection of major problems in urban planning and management (Zhao et al., 2023; Shen & Zhang, 2024; Zhang et al., 2019). The use of satellite remote-sensing data for specific wavelength invertion can accurately collect surface temperature, humidity and atmospheric environmental quality, and then match and correct the scale with the data from the ground monitoring system, so that various climate-element indicators can be obtained at different scales.

In the proposed planning framework, representative indicators of different types of climate elements were selected. The calculation method and data source of each indicator are listed in Table 1. The indicators were visually represented and standardised in GIS as the data basis for establishing correlation matrices with urban morphology parameters.

Table 1. Calculation method and data sources for urban climate factor.

Level 1	Level 2	Meaning of climate elements	Calculation methodology,data sources and time
Micro-climate elements	LST	A key parameter for the exchange of matter and energy between the surface and the atmosphere. (Wu et al., 2023)	$\mathrm{FVC} = \frac{\mathrm{NDVI} - \mathrm{NDVI_{siol}}}{\mathrm{NDVI_{veg}} - \mathrm{NDVI_{siol}}}$ $\varepsilon = 0.004\mathrm{FVC} + 0.986$ $L_r = \varepsilon \times \tau \times B(T_s) + (1-\varepsilon) \times \tau \times L_D \downarrow + L_u \uparrow$ $\mathrm{B}(\mathrm{T_s}) = \frac{\mathrm{L_r} - L_u \uparrow - (1-\varepsilon) \times \tau \times L_D \downarrow}{\varepsilon \times \tau}$ $T_s = \frac{K_2}{\ln\left[\frac{K_1}{B(T_s)} + 1\right]}$ Where, FVC denotes the vegetation cover. NDVI denotes the normalised vegetation index. $\mathrm{NDVI_{soil}}$ denotes the normalised vegetation index for areas without vegetation cover. $\mathrm{NDVI_{veg}}$ denotes the normalised vegetation index for areas with full vegetation cover and ε denotes the surface-specific emissivity from the Landsat 8 OLI_TIRS satellite sensor. Where, is thermal infrared radiation brightness values. We obtained the atmospheric calibration parameters (atmospheric transmittance τ, atmospheric upgoing radiance Lu↑ and atmospheric downgoing radiance LD↓) for the Landsat sensor from the NASA website. T_s is LST and K_1 and K_2 are preset parameters.
	WET	Humidity reflects the moisture content of water bodies, soil and vegetation. It is closely related to the ecological environment (Shi et al., 2022)	$\mathrm{WET} = 0.1509\rho_{BLUE} + 0.1973\rho_{GREEN} + 0.3279\rho_{RED} + 0.3406\rho_{NIR} - 0.7112\rho_{SWIR1} - 0.4572\rho_{SWIR2}$ Where, ρ denotes the spectral reflectance of the corresponding band.
	Uz	The local wind speed change in urban micro-climates produces variations in height and is influenced by the local environment roughness length（Ku et al., 2020）	$U_z = \frac{u_*}{K}\ln\left(\frac{z}{z_0}\right)$ Where Uz denotes the average wind speed at a height Z above the ground, set to 1.5 m in this study, U* denotes the friction velocity, K is Kamen's constant-generally approximated as 0.4—and Z_0 denotes the aerodynamic roughness length.

Atmospheric elements	$PM_{2.5}$	Fine particulate matter is an important index for measuring and controlling air pollution levels.	$PM_{2.5}$ Asia data at 0.01° × 0.01° resolution made publicly available at Washington University. (https: //sites. wustl. edu/acag/datasets/surface-pm2-5/)
	CO_2	A carbon—oxygen compound that is a common greenhouse gas.	Open Data Inventory of Anthropogenic Carbon Dioxide, a high spatial resolution global dataset of carbon dioxide emissions. (https://db.cger.nies.go.jp/dataset/ODIAC/DL_odiac2024b.html)

3.2. Analysis of the Correlation Between Urban Morphology and Climate Elements

The prerequisite for establishing the correlation between urban morphology and climate elements is the existence of spatial stratified heterogeneity in the distributional characteristics of the two, which is used to describe geographic phenomena in which the variance within a stratum is smaller than the variance between strata and is mainly applied to geospatial, climatic zoning and urban—rural differences (Pickett et al., 2017). Indicators of urban climate elements and urban morphology parameters are typical geospatial data; there is a certain spatial dependence between data samples, and statistically significant analysis results can be obtained by establishing of regression models. Commonly used regression models include classical linear regression, nonlinear regression, and spatial regression models etc (Dorigon & Amorim, 2019; Xiao et al., 2018). The determination of urban morphology parameters involves two steps: ①the parameters are first determined based on existing urban morphology parameters affecting the urban climate environment. ②Next, combining with the distribution characteristics of multiple climate-element indicators in Shenyang, the indicators are screened through the autocorrelation analysis between indicators. The final urban morphology parameters are listed in Table 2. The data of urban morphology parameters were obtained from remote-sensing images of a 196.96-km² administrative area, with a 200m × 200-m² spatial grid as the statistical unit.

Table 2. Description calculation of urban morphology parameters.

Urban morphology parameters	**Description**	**Calculation method**
ISF	Impervious percentage of the plot; range: 0—1	$$ISF = \frac{(\rho_{MIR} - \rho_{NIR})}{(\rho_{MIR} + \rho_{NIR})}$$ ρ_{MIR} denotes the mid-infrared band and ϱ_{NIR} denotes the near-infrared band.
RND	Ratio of road network length to road network area; range: 0—1	$$RND = \frac{L_{bn}}{A_{ta}}$$ L_{bn} denotes the length of the road network in the region and A_{ta} denotes the total area of the region.
NDVI	Ratio of vegetation vertical projection area to plot area; range: —1 to 1	$$NDVI = \frac{(\rho_{NIR} - \rho_{RED})}{(\rho_{NIR} + \rho_{RED})}$$ ρ_{NIR} denotes the mid- and near-infrared bands and ϱ_{RED} denotes the red-light band.
BH	Average building height; range: 0—∞	$$BH = \sum_{i=1}^{n} Hi$$ H_i is the average height of buildings in the region.

 doi:10.20944/preprints202604.0445.v1

BD	Ratio of building footprint to plot area; range: 0—1	$BD = \frac{A_{bb}}{A_{ta}}$ A_{bb} is the building footprint and A_{ta} is the total area of the region.
SVF	Sky visibility at a point on the surface of the unit; range: 0—1	$SVF = 1 - \sum_{i=0}^{n} \sin^2 \beta \times (\frac{\alpha}{360})$ α is the azimuth angle, β is the maximum building height angle within the sector of the corresponding azimuth angle within the study radius. n = 360/α; α should not be >10°, and R should not be <20.

3.3. Urban Morphology Design Based on Multi-Objective Optimisation of Climate Elements

The essence of the optimal design of urban morphology oriented towards multiple climate elements is to morphology the most scientific and optimal spatial element configuration around multiple urban ecological processes. Urban morphology drives multiple ecological effects. Different patterns and elemental compositions have different impacts on specific ecological effects. Considering the goal of fine governance and high-quality development, achieving a balanced effect of urban morphology on multiple climate elements and synergistic optimisation of water, soil, atmosphere and biodiversity, as well as realising the optimal ecological service function in artificial environments are core aspects mainly addressed in this study. Multi-objective programming, which entails optimising multiple objectives for a given area simultaneously, has been applied to urban ecological service function trade-offs, siting of public service facilities and other tasks (Chen et al., 2023; Guo et al., 2022; Zhang et al., 2022). The SPEA-2 algorithm is a multi-objective optimisation method based on evolutionary algorithms used to optimise multiple objective functions (≥2) satisfying certain constraints as follows:

$$\min[f_1(x), f_2(x), \ldots, f_m(x)]$$

$$s.\ t.\ \begin{cases} Lb \le x \le ub \\ Aeq \times x = beq \\ A \times x \le b \end{cases}$$

where $f_i(x)$ denotes the objective function to be optimised; x is the variable to be optimised; $1b$ and ub are the lower and upper bound constraints on the variable x, respectively; $Aeq \times x = beq$ is the linear equation constraint on the variable x and $A \times x \le b$ is the linear inequality constraint on the variable x.

Multi-objective optimisation problems require each sub-objective to be optimal (ideal solution). In addition to optimising each objective, it is also necessary to balance the relationship between objectives. The optimisation result is often a set of Pareto-optimal solutions obtained after trade-offs between the objectives rather than a unique solution.

4. Analysis of the Correlation Between Urban Climate Elements and Urban Morphology in Shenyang City

4.1. Study Area

Shenyang (41°48′11.75″N, 123°25′31.18″E) is located in the northern cold climate zone and is the only megacity in northeastern China. It has a temperate semi-humid continental climate. There are four distinct seasons with an average annual temperature of 6.2℃–9.7℃. This study considers the main urban area of Tiexi, Shenyang City, with a total area of 196.96 km^2(Figure 2).

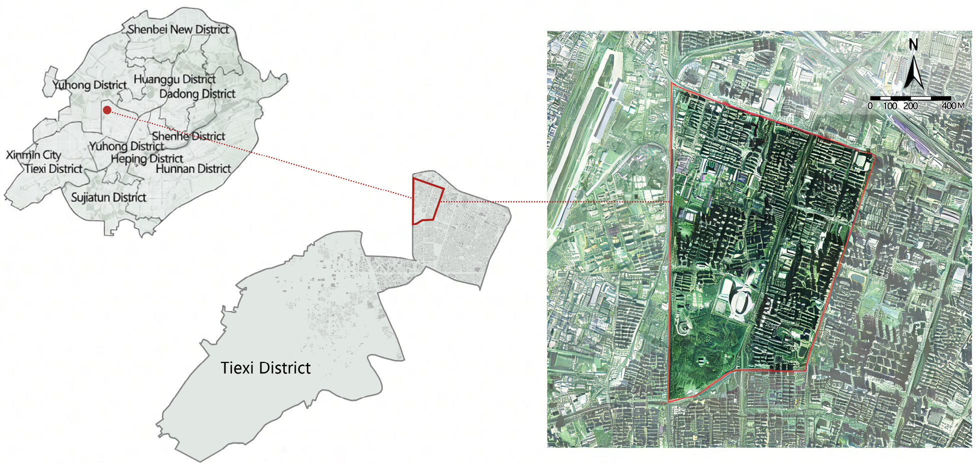

Figure 2. Location map of demonstration area.

4.2. Characteristics of Spatial Distribution of Climate Elements in Shenyang

Multi-source remote-sensing imaging and monitoring data were used to quantify multiple climate-element indicators in Tiexi, Shenyang City (Table 1). The spatial grid of 200m × 200 m² was used as the statistical unit to realise the spatial visual expression of multiple climate-element indicators (Figure 3).

In terms of the distribution pattern of climate elements, spatial heterogeneity is characterised significantly. The three indicators of the micro-climate elements showed spatial variations with a pronounced granularity at the 200 × 200-m² raster resolution, indicating that parameters such as spatial morphology and sub-surface characteristics within the raster are very sensitive to the micro-climate elements. The spatial variation and granularity of the atmospheric environmental elements were significantly larger than that those of other elements, indicating a trend of high centre, low periphery and decreasing circles at the urban scale, with insignificant differences in the indicators in each grid in the local area. This result was attributed to the different data sources and the number of monitoring sites, and indicated that due to the mobility characteristics of the gases, they are less sensitive to spatial patterns than other climatic elements, and are more influenced by the type of land use, the source of emissions and structural characteristics at the urban scale. The above analysis of the spatial distribution characteristics and scales of multiple climate elements in Tiexi, Shenyang City, shows that the urban morphology is spatially stratified and heterogeneous, driving the urban multiple climate elements to show different spatial distribution patterns.

In terms of climate-element indicator levels, surface temperature morphology large areas of high values. It is widely distributed and contiguous within the central city and western industrial area, which is prone to the risk of high-temperature heat waves. Humidity is lowest in the built-up land between the second- and third-ring roads, which is related to the increase in the total amount of development and construction, which has changed the surface circulation process. The local wind speed difference is large, and under the same background meteorological conditions, the local wind speed difference between the suburban open area and high-density central area can reach 2.5 m/s, which also indirectly affects the surface cooling and pollutant gas diffusion in the central area of the city. The concentration indices of the two gases in the atmospheric environmental elements differ seasonally; however, they both have concentration elements in urban centres. The high value area of the distribution of climate-element indicators in Tiexi, Shenyang City will be considered as the focus space for optimisation, and further regulation counter-measures will be sought in terms of the correlation with urban morphology.

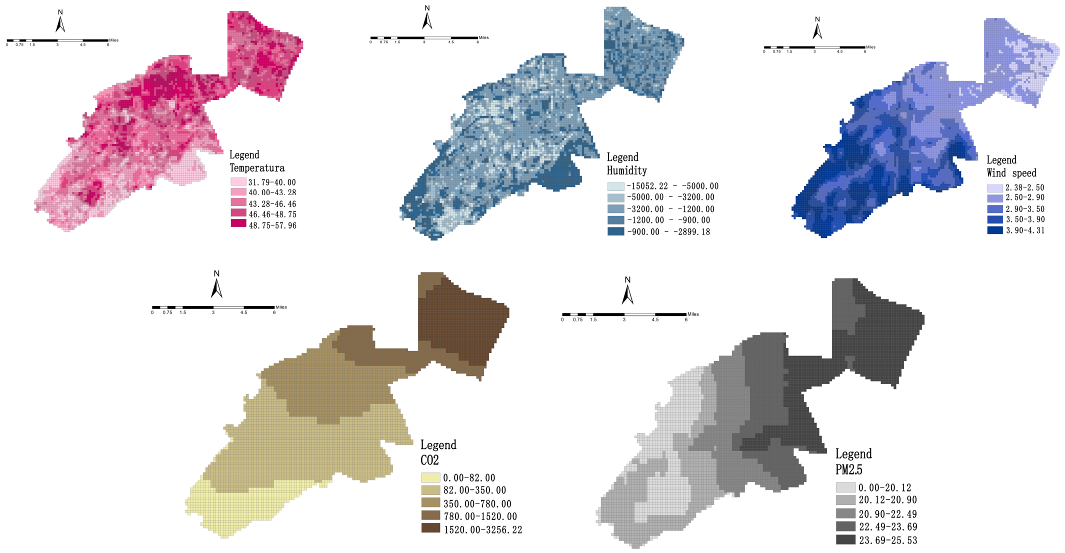

Figure 3. Spatial distribution of indicators of climate elements in Tiexi, Shenyang City.

To ensure the accuracy of the climate-element indicators in this study, the above climate-element indicators were validated. The concentration values of the two gases in the atmospheric elements are measured data from meteorological stations; thus, the surface temperature, humidity and wind speed indicators obtained using remote-sensing inversion are mainly verified. Data from the Shenyang Meteorological Monitoring Station and inversion results were used for validation. The comparison results are shown in Figure 4, and the inversion values of the three elemental indices are consistent with the trend of the measured values, with high accuracy.

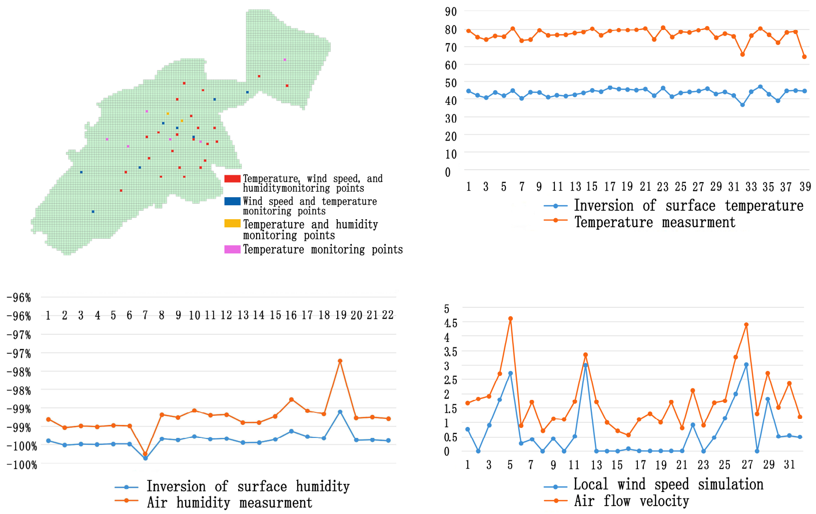

Figure 4. Comparison of the simulated and measured values.

4.3. Regression Analysis of Climate Elements and Spatial Patterns in Shenyang City

The regression analysis of Shenyang City's climate elements and urban morphology is performed, the sensitive parameters of urban morphology are screened as variables, and a regression model with the indicators of climate elements is established. The mechanism of the effect of urban morphology on climate elements is revealed, and the synergistic optimisation of multiple climate elements in the city is realised from spatial planning.

 doi:10.20944/preprints202604.0445.v1

First, the morphological parameters representing different aspects of buildings, sub-surface and spatial relationship were selected, and the convergent indicators were excluded through covariance analysis by applying SPSS software. The correlation analysis between the indicators of climate elements and morphological parameters of Shenyang City was performed, and the Pearson correlation coefficients and significance were compared as the basis for the screening variables. Morphological parameters that are significantly correlated with each other at $P < 0.005$ are selected as regression variables from a wide range of indicators, i.e., building height (BH), building density (BD), sky view factor (SVF), impervious surface fraction (ISF), normalised difference vegetation index (NDVI) and road network density (RND). Second, the regression model of different indicators of climate elements and morphological parameters in Shenyang City was established. The standardised coefficient R^2 was used to explain and compare the influence of each morphological parameter on multiple climate elements and determine its degree of contribution.

Both urban climate element indicators and urban morphology parameters are typical geospatial data. Considering that the traditional regression analysis is based on the observation independence assumption, the spatial dependence of the urban built environment is ignored. In this study, the influence of spatial location was considered, and the spatial lag model (SLM) and spatial error model (SEM) in the spatial regression model analysis software GeoDa were used to analyse the spatial influences of multiple climate elements in Shenyang City and establish the regression models of the different climate elements and morphological parameters in Shenyang City. The Lagrange multiplier (LM) and robust Lagrange multiplier (R-LM) indices were introduced and tested in GeoDa software. Larger and more significant LM and R-LM values for a particular spatial regression model indicate more suitable. From the results, the temperature, humidity and wind speed were modelled optimally with SEM and $PM_{2.5}$ and CO_2 were modelled optimally with SLM (Table 3).

Table 3. Space dependence diagnosis of the LM method.

	LM(lag)	**R-LM(lag)**	**LM(error)**	**R-LM(error)**
LST	4023.4105	313.1859	5677.6176	1967.3930
WET	2843.3644	176.8633	3433.0371	766.5360
U_z	1570.4769	390.6776	1963.7946	683.9953
CO_2	10859.9480	2221.2751	9776.0030	1137.3301
$PM_{2.5}$	94.3167	40 7928	54. 8377	1.3137

The regression models of the five climate element indicators and each influencing factor are shown in Table 4. From the regression results, R^2 has a high level (0.68–0.99), which also indicates that the distribution of the climate elements has an obvious spatial dependence.

Table 4. Regression results of SLM and SEM.

Implicit variable	**Variant**	**Constant**	**BH**	**BD**	**ISF**	**NDVI**	**SVF**	**RND**
LST	Modulus	0.418	0.004	0.302	0.105	-0.183	0.038	0.038
	P-value	0.000	0.582	0.000	0.000	0.000	0.000	0.000
	Selected Models	SEM						
	R^2	0.85						
	LL	8533.98						
	AIC	-17053.9						
	SC	-17007.7						
WET	Modulus	0.575	-0.089	-0.493	0.107	0.218	-0.102	-0.013

	P-value	0.000	0.000	0.000	0.000	0.000	0.000	0.175
	Selected Models				SEM			
	R^2				0.68			
	LL				-44957.53			
	AIC				89929.1			
	SC				59975.3			
	Modulus	-0.077	-0.819	0.101	-0.076	0.052	0.755	-0.073
	P-value	0.001	0.000	0.000	0.000	0.003	0.000	0.000
	Selected Models				SEM			
U_Z	R^2				0.87			
	LL				-2842.13			
	AIC				5698.26			
	SC				5744.48			
	Modulus	0.013	-0.008	-0.003	-0.002	-0.001	-0.016	0.008
	P-value	0.000	0.000	0.000	0.178	0.751	0.000	0.000
	Selected Models				SLM			
CO_2	R^2				0.99			
	LL				4472.94			
	AIC				-8929.88			
	SC				-8888.19			
	Modulus	0.973	0.026	-0.219	-0.064	-0.162	-0.383	0.179
	P-value	0.000	0.661	0.000	0.080	0.001	0.000	0.000
	Selected Models				SLM			
$PM_{2.5}$	R^2				0.99			
	LL				3153.71			
	AIC				-6293.43			
	SC				-6256.95			

The absolute value of the regression coefficients reflects the degree of influence of each morphological variable on the indicators of each climate element. The degree of influence of the morphological parameters on the various climate elements is counted separately (Figure 5), which serves as a basis for regulating the climate elements in the planning application below, is quantified separately (Figure 4).

Through regression analysis, a previous study proved that the distribution of climate elements in Shenyang City is spatially aggregated and there is spatial autocorrelation. A spatial regression analysis model was constructed with six morphological parameters screened as variables. The model results can explain the (1) effect of urban morphology parameters on different climate elements under the combination of multiple variables and (2) the degree of influence of each specific morphology parameter on climate elements under the joint action of multiple elements. Hence, to explore the necessary quantitative analysis basis for optimising climate elements in Shenyang City from the spatial planning approach, the multi-objective synergistic optimisation of climate elements was further combined with specific urban regeneration plots.

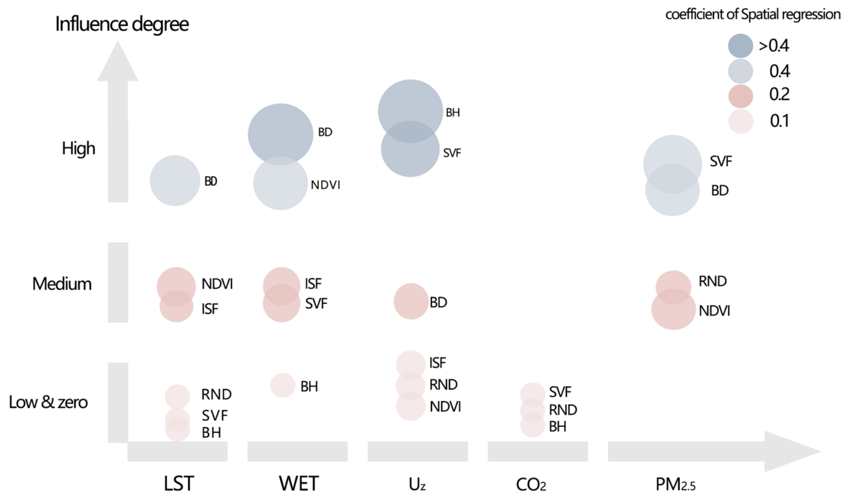

Figure 5. Influence of morphological parameters on climatic elements in Shenyang City.

5. Application of Multi-Objective Optimisation of Climate Elements in Typical Areas of Shenyang City

5.1. Multi-Objective Optimisation Algorithm and Parameter Setting

We construct a multi-objective optimisation model for the climate-element indicators. The regression function of the single climate-element indicators in this study adopts multi-variate linear regression, and the function variables correspond to the urban morphology parameters. The planning and design programme determines the range of values of the variables (Table 5).

The modelling algorithm is based on the Improved Pareto Intensity Evolutionary Algorithm (SPEA-2 algorithm) built into the Grasshopper platmorphology call plugin, Octopus. Using the above six urban morphological parameters as independent variables, the models were plugged into the Genome side (variable side) of the Octopus operator. Multiple climate-element indices were used as optimisation objectives, which were plugged into the objective side of the Octopus operator and solved separately. In the target value setting, humidity was targeted at the maximum value, and the other indices were targeted at the minimum value (Table 3). After obtaining the optimisation results, the standardised data results are reduced to values with practical significance.

Table 5. Multi-objective optimisation model.

Optimisation elements	Function name	Function	R^2	Unit	Range of values
Micro-climate elements	Surface temperature regression function	$Y=0.013X_1+13.03X_2+3.89X_3-5.67X_4-5.33X_5+7.77X_6+32.638$	0.648	℃	
	Surface moisture regression function	$Y=-27.95X_1-9106.23X_2+1206.96X_3+3161.45X_4+32675.24X_5-7895.61X_6-917.89$	0.53	—	X_1 [0–91.5] X_2 [0.18–0.85]
	Local wind speed regression function	$Y=-0.038X_1-0.004X_2-0.35X_3+0.19X_4-6.05X_5+5.86X_6-3.23$	0.841	m/s	X_3 [0.4–1] X_4 [0.18–0.80]
Atmospheric environmental elements	CO_2 regression function	$Y=-18.39X_1-1022.80X_2+215.38X_3-119.64X_4+41413.57X_5-5412.93X_6+5520.50$	0.654	t	X_5 [0.77–0.82] X_6 [0–0.03]
	$PM_{2.5}$ concentration regression function	$Y=-0.034X_1-3.07X_2-1.21X_3-8.73X_4+93.93X_5+3.90X_6+24.56$	0.506	ug/m^3	

 doi:10.20944/preprints202604.0445.v1

where X_1 represents BH,X_2 represents BD,X_3 represents ISF,X_4 represents NDVI,X_5 represents SVF,and X_6 represents RND.

5.2. Analysis of Optimisation Results

In the experiment, the simulation process stabilised the population state after 20 iterations, and the results are shown in Figure 6. The red dots in the coordinate system indicate the most recent generation of elite solutions. It can be seen from the process of generating the solution set that the line of the most recent generation of elite solutions close to the origin of the coordinate origin is the Pareto frontier solution set, and as the number of iterations increases, the solution set of the scheme gradually converges to the Pareto frontier. Through data comparison and analysis, the following conclusions can be drawn. In this demonstration area, the optimisation indices of the climate elements exhibited a linear relationship, which coincides with the relationship established between the indicators of climate-elements and spatial morphology parameters.

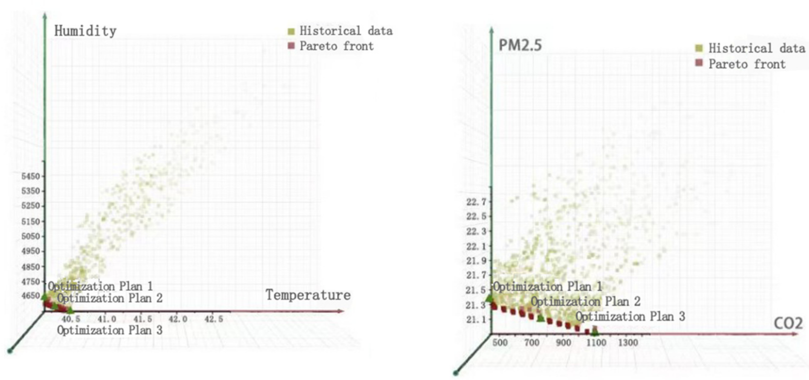

Figure 6. Octopus results.

Table 6. Octopus-related parameter setting table.

Parameter	Population Size	Max Generation	Elitism	Mutation Probability	Mutation Rate	Crossover Rate
Reference point	100	20	0.5	0.2	0.9	0.8

Because the Pareto solution is a set of better solutions, in the planning and design of urban renewal, the combination of morphological parameters with lower cost should be selected with the objective of optimisation of climatic elements by combining the current situation. As there are more climate-element indicators and different optimisation objectives, we select the optimal solution sets of micro-climate elements and atmospheric environment elements, then seek their intersection and finally determine the solution set of urban morphology parameters with multi-factor synergy (Figure 7).

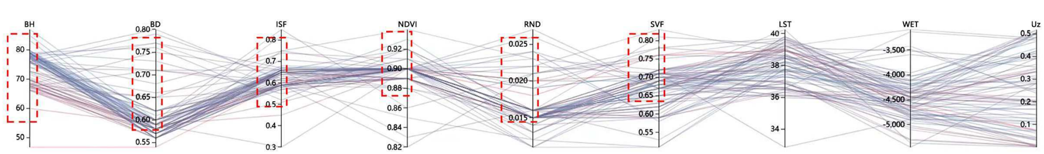

(a)

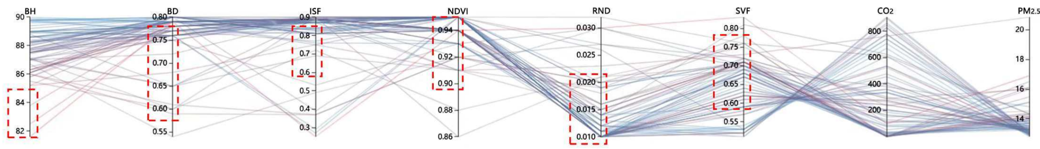

(b)

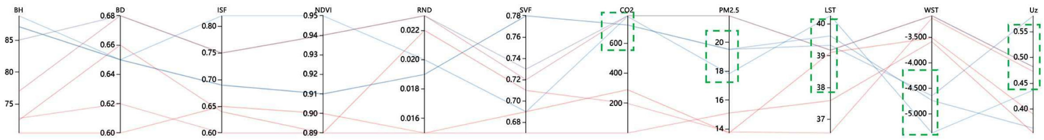

(c)

Figure 7. a)Optimal set of solutions for the micro-climate elements for each variable.b)Optimal set of solutions for each variable for the atmospheric environmental factors. c) Optimal set of solutions for a variable based on intersection.

5.3. Optimisation Programme

In the urban renewal programme design, the land parcel is divided into 28 rasters and the morphological parameters of each raster are extracted. The planning and design scheme of the demonstration area (Figure 8) is based on the aforementioned optimal solution set to determine the range and regulation strategy of the urban morphological parameters (Table 7). As the region is an old urban region, which is characterised by a high BD and low BH, the development intensity of the site is increased during the optimisation of building morphology. Further, the BH is increased appropriately in some parcels to save a part of the site for constructing public green space and to improve the urban permeability of the region via the morphology optimisation; the saved part includes 10 parcels. In green space system optimisation, a green ecological network based on road greening and a central green space is employed. In sub-surface optimisation, some hard surfaces are retrofitted with permeable tiles, which substantially increases the proportion of permeable surfaces in the region.

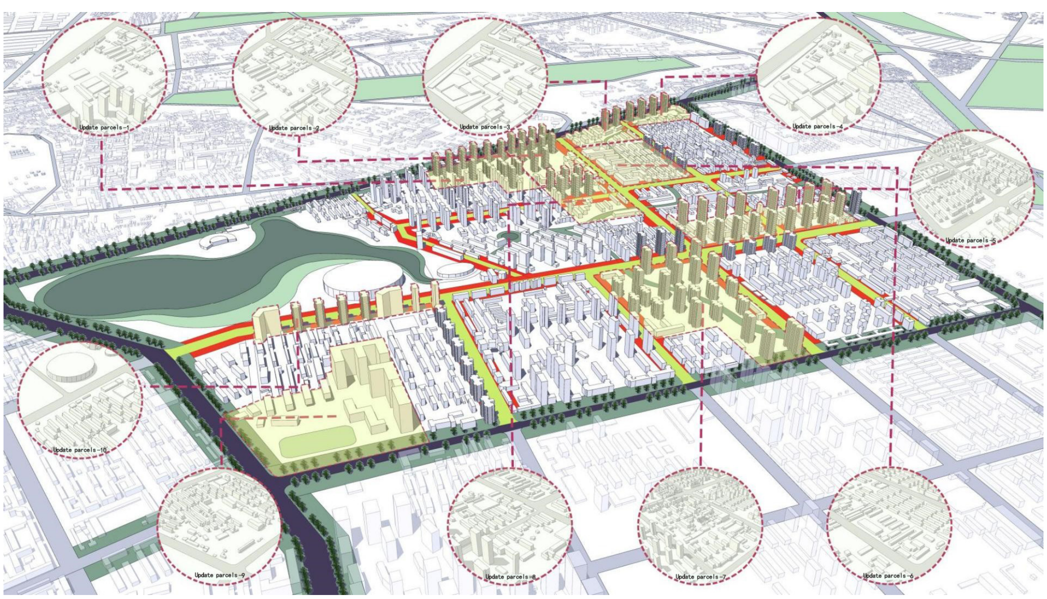

Figure 8. Multi-objective Optimisation of Climate elements in demonstration areas.

Table 7. Multi-objective Optimisation of climate elements in urban renewal demonstration zones.

Classification	Morphological indicators	Appropriate interval	Effect	Regulatory principles	Planning methodology
Surface cover indicators	ISF	0.60–0.85 is desirable	Significant: None Fair: LST,WET Less significant: U_Z	1. Reduce the radiant heat flux received and reflected by the ground surface and alleviate the uneven heating of the ground; 2. Increase the permeability of the ground surface to regulate temperature and humidity through transpiration.	1. Increase the green space ratio of the underlayment; 2. Use permeable materials for hard surfaces where it is not possible to increase the green space.
	NDVI	Optimised in the range 0.9-1.0	Significant:WET Fair: LST, $PM_{2.5}$ Less significant: U_Z	1. Humidity and temperature are regulated through transpiration by plants; 2. Regulate through the ability of plants to adsorb atmospheric particulate matter; 3. Increase the open space to improve ventilation.	1. The principle of large concentrations and small dispersions; 2. Increase the amount of greenery at every-turn; 3. The use of large canopy trees and related layout techniques.
	RND	0.010–0.026 is desirable	Significant:None Fair: $PM_{2.5}$ Less significant: LST, U_Z, CO_2	1. Reduce harmful emissions from motor vehicles; 2. Reduce the proportion of hard surfaces; 3. Integrate the heat gain and heat loss from the underlayment.	1. 700m≤main road spacing≤1200m 2. 300m≤spacing of secondary roads≤500m
	BH	Under the premise of ensuring the floor area ratio, it is appropriate to control 55–85m	Significant: U_Z Fair: None Less significant: LST, WET, CO_2	1. Increase urban roughness and alter localised wind fields; 2. Shade solar radiation by buildings and affect localised temperature and humidity; 3. Change the height of the urban canopy, affecting the vertical distribution of CO_2.	1. Use combination of high-rise towers and ground-floor buildings; 2. Develop a staggered layout of high-rise buildings wherever possible; 3. Avoidance of unimorphologyity of height and varied skylines.

Construction intensity indicators	BD	0.58–0.78 is desirable	Significant: LST, WET, $PM_{2.5}$ Fair: U_Z Less significant: CO_2	1. Increasing the building cover and altering the energy and water–air cycle at the surface; 2. Increase anthropogenic heat emissions and atmospheric particulate emissions; 3. Reduce the permeability of the city, affecting wind fields.	1. Moderate increase in the average building height when the plot ratio is certain; 2. Use a combination of high-rise towers and ground-floor buildings.
Building morphology indicators	SVF	0.68–0.78 is desirable	Significant: U_Z, $PM_{2.5}$ Fair: WET Less significant: LST, CO_2	1. Increase the breathability of the city; 2. Combine open and green space to regulate temperature and humidity; 3. Improve ventilation and facilitate the diffusion of pollution gases.	1. Appropriately reduce the street height-to-width ratios; 2. Areas with high building densities or heights should be staggered as much as possible.

doi:10.20944/preprints202604.0445.v1

To compare the enhancement of the climate-element indicators of the area as a whole, we comprehensively calculate the average value of each raster climate element before and after optimisation (Figure 9). All five climate-element indicators produced significant changes. Among the micro-climate elements, the mean surface temperature decreased from 42.8℃ to 40.3℃. The surface humidity index increased from -7840 to -6354. The local wind speed only improved from 'no wind' to 'soft wind' due to the original low wind speed. Among the atmospheric factors, the CO_2 concentration index decreased significantly from 1632.9t/km² to 936.5t/km², and the $PM_{2.5}$ concentration decreased from 23.4ug/m³ to 20.2ug/m³. Except for the wind speed, which had a low original value and a relatively wide optimisation range, the optimisation range of the other climatic factors was 6.5%–42.6%. This shows that if the programme is implemented, the multiple climate-element indicators can be improved and optimised in a more balanced manner.

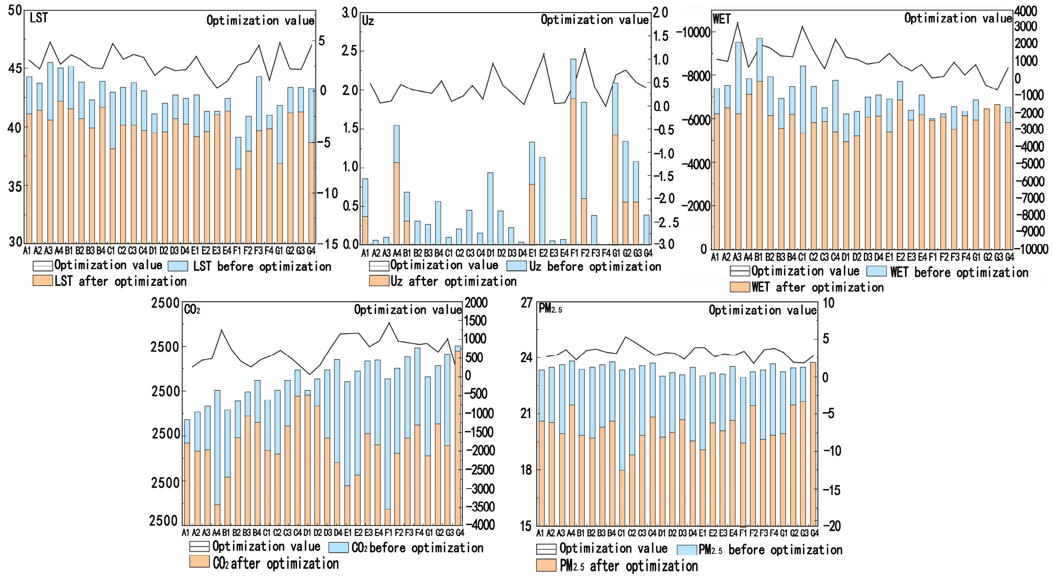

Figure 9. Indicator set of current and planned spatial patterns and climate elements in the demonstration area.

6. Conclusions and Outlook

Herein, we explored the influence of urban morphology on climate elements in Shenyang City. Notably, spatial and temporal changes in the two factors may affect their relationship. In future studies, we will observe long time-series climate dynamics in more depth to accurately study these variations and their effects. Urban spatial patterns exhibit diversity and complexity, and the relationship with climate elements has obvious scale effects, which makes it difficult to derive patterns from limited observation samples. The use of machine learning methods helps to handle non-linear relationships between response and independent environmental variables. This development will be a refinement and supplement to the present method.

We established a statistical model and explored the coupling relationship between urban morphology and climate element. Further, we proposed a multi-objective optimisation method for urban climate elements. The results show that the R^2 value of the spatial regression model was high (0.68–0.99), indicating that the model can better reveal the relationship between urban morphology parameters and climate elements. The BD, NDVI, ISF and SVF were identified to be the common indicators of micro-climate elements. Further, the RND and SVF were identified to be the common indicators of atmospheric elements. The interaction analysis between urban morphology parameters and climate elements was performed using a parametric model, and the genetic algorithm was used to solve a set of multiple regression equations to obtain the Pareto-optimal urban morphology. The optimisation range of several climate-element indicators was 6.5%–42.6%.

 doi:10.20944/preprints202604.0445.v1

Notably, a quantitative approach was used herein to clarify the moderating role of urban morphology on climate elements. In traditional studies, urban morphology is often used to explain differences in climate environments, such as the more typical local climate zoning method, but it is not possible to quantify specific planning indicators. Regression analysis can provide a basis for determining planning indicators in the study area according to current climatic environment, which can be adapted to local conditions. Various specialised plans are often targeted to address specific urban issues, such as urban ventilation corridor planning, and fewer plans consider the synergistic optimisation of multiple climatic elements in an integrated manner. Urban space drives multiple climate processes, and climate elements interact with each other. Therefore, it is essential to consider multiple climate issues by optimising the urban morphology to develop an actionable method of planning and design to enhance the climate resilience of cities—an aspect considered in this study.

References

1. Inostroza, L.,&Zepp,H.(2021). The metabolic urban network:Urbanisation as hierarchically ordered space of flows. Cities, 109. https://doi.org/10.1016/j.cities.2020.103029.
2. Inostroza, L.(2018). The circularity of the urban ecosystem material productivity: The transmorphologyation of biomass into technomass in Southern Patagonia. Sustainable Cities and Society, 39, 335–343.https://doi.org/10.1016/j.scs.2018.03.001.
3. Krueger,E.H.,Constantino, S.M., Centeno,M.A., Elmqvist, T., Weber,E.U.,&Levin, S.A.(2022).Governing sustainable transmorphologyations of urban social-ecological-technological systems. Npj Urban Sustainabilty, 2(1). https://doi.org/10.1038/s42949-022-00053-1.
4. Fu, B.J., Zhao, W.W., Chen, L.D., Lu, Y.H.,&Wang, D. (2006). A multiscale soil loss evaluation index. Chinese Science Bulletin, 51(4), 448–456. https://doi.org/10.1007/s11434-006-0448-2.
5. Ferguson, G.,&Woodbury, A.D. (2007). Urban heat island in the subsurface. Geophysical Research Letters, 34(23). https://doi.org/10.1029/2007GL032324.
6. Taniguchi, M., Burnett, W.C.,&Ness, G.D.(2008). Integrated research on subsurface environments in Asian urban areas. Science Of The Total Environmental, 404(2-3), 377–392. https://doi.org/10.1016/j.scitotenv.2008.04.033.
7. Tsirigoti, D.,&Tsikaloudaki, K. (2018). The Effect of Climate Conditions on the Relation between Energy Efficiency and urban morphology. Energies, 11(3). https://doi.org/10.3390/en11030582.
8. Ke,X.L., Wang,X.Y., Guo,H.X.,Yang,C.Zhou,Q.,&Mougharbel,A. (2021). Urban ecological security evaluation and spatial correlation researchbased on data analysis of 16 cities in Hubei Province of China. Journal Of Cleaner Production, 311. https://doi.org/10.1016/j.jclepro.2021.127613.
9. Yang, M.,Jiao, M.Y.,&Zhang,J.Y.(2022). Coupling Coordination and Interactive Response Analysis of Ecological Environment and Urban Resilience in the Yangtze River Economic Belt. Internationl Journal Of Environmental Research And Public Health, 19(19). https://doi.org/10.3390/ijerph191911988.
10. Shi, C.C, Guo, N.L., Zeng, L.L.,&Wu, F. (2022). How climate change is going to affect urban livability in China. Climate Services, 26. https://doi.org/10.1016/j.cliser.2022.100284.
11. Gao, B.P., Wu, Y.M., Li, C., Zheng, K.L.,&Wu, Y. (2022). Ecosystem Health Responses of Urban Agglomerations in Central Yunnan Based on Land Use Change. Internationl Journal Of Environmental Research And Public Health, 19(19). https://doi.org/10.3390/ijerph191912399.
12. Guenette, S., Araujo, J.N.,&Bundy, A. (2014). Exploring the potential effects of climate change on the Western Scotian Shelf ecosystem. Journal Of Marine Systems, 134, 89–100. https://doi.org/10.1016/j.jmarsys.2014.03.001.
13. He, X.Y., Liang, J., Zeng G.M., Yuan Y.J., &Li, X.D. (2019). The Effects of Interaction between Climate Change and Land-Use/Cover Change on Biodiversity-Related Ecosystem Services. Global Challenges, 3(9). https://doi.org/10.1002/gch2.201800095.
14. Christensen, N.L., Brown, J.H., Carpenter, S., Dantonio, C., Francis, R., Franklin, J.F., Macmahon, J.A., Noss, R.F., Parsons, D.J., Peterson, C.H., Turner, M.G., Woodmansee, R.G., &Bartuska AM. (1996). The report of the ecological society of america committee on the scientific basis for ecosystem management . Ecological Applications, 6(3).

 doi:10.20944/preprints202604.0445.v1

15. Schmitz, O.J., Post, E., Burns, C.E., &Johnston, K.M. (2003). Ecosystem responses to global climate change: Moving beyond color mapping. Gbioscience, 53(12),1199–1205. https://doi.org/10.1641/0006-3568(2003)053[1199:ERTGCC]2.0.CO;2.
16. Grimm, N.B., Groffman, P., Staudinger, M.,&Tallis, H.(2016). Climate change impacts on ecosystems and ecosystem services in the United States: process and prospects for sustained assessment. Climate Change, 135(1), 97–109. https://doi.org/10.1007/s10584-015-1547-3.
17. Luccioni, A., Schmidt, V., Vardanyan, V.,&Bengio, Y.(2021). Using Artificial Intelligence to Visualize the Impacts of Climate Change. Ieee Computer Graphics And Applications, 41(1), 8–14. https://doi.org/10.1109/MCG.2020.3025425.
18. Mohamed, O.Y.A.,&Zahidi, I.(2024). Artificial intelligence for predicting urban heat island effect and optimising land use/land cover for mitigation: Prospects and recent advancements.Urban Climate,55. https://doi.org/10.1016/j.uclim.2024.101976.
19. Zhao, J., Guo, F., Zhang, H.C.,&Dong, J.(2024). Mechanisms of non-stationary influence of urban morphology on the diurnal thermal environment based on machine learning and MGWR analysis. Sustainable Cities and Society, 101. https://doi.org/10.1016/j.scs.2024.105194.
20. Jiang, Y.F., Han, X.M, Shi, T.M.,&Song, D.R.(2019). Microclimatic Impact Analysis of Multi-Dimensional Indicators of Streetscape Fabric in the Medium Spatial Zone. International Journal Of Environmental Research And Public Health, 16(6). https://doi.org/10.3390/ijerph16060952.
21. Othman, H.A.S.,&Alshboul, A.A. (2020). The role of urban morphology on outdoor thermal comfort: The case of Al-Sharq City-Az Zarqa. Urban Climate, 34. https://doi.org/10.1016/j.uclim.2020.100706.
22. Oke, T.R.,&Canada.(2004). Initial guidance to obtain representative meteorological observations at urban sites. Geneva: World Meteorological Organization, 51.
23. Shao, L.D., Liao, W.L., Li, P.L., Luo,M., Xiong, X.H.,&Liu, X.P.(2023). Drivers of global surface urban heat islands: Surface property, climate background, and 2D/3Durban morphologies. Building And Envieonment, 242. https://doi.org/10.1016/j.buildenv.2023.110581.
24. Li, Y., Schubert, S., Jürgen P.Kropp,&Rybski, D.(2020). On the influence of density and morphology on the urban heat island intensity. Nature Communications, 11, 1-9. https://doi.org/10.1038/s41467-020-16461-9.
25. Feng, Yang, Liang,&Chen. (2016). Developing a thermal atlas for climate-responsive urban design based on empirical modeling and urban morphological analysis. Energy&Buildings. https://doi.org/10.1016/j.enbuild.2015.11.047.
26. Kubota, T., Miura, M., Tominaga, Y.,&Mochida, A. (2008). Wind tunnel tests on the relationship between building density and pedestrian-level wind velocity: development of guidelines for realizing acceptable wind environment in residential neighborhoods. Building and environment, 43(10), 1699-1708.
27. Sharag-Eldin, A.(2007). A parametric model for predicting wind-induced pressures on low-rise vertical surfaces in shielded environments. Solar Energy, 81(1), 52-61. https://doi.org/10.1016/j.solener.2006.06.007.
28. Zhang, S., Fang, X.Y., Cheng, C., Chen, L.X., Zhang, L., Yu, Y., Li, L.,&Luo, H.Y. (2022). Research on the Planning Method and Strategy of Urban Wind and Heat Environment Optimization-Taking Shenzhen, a Sub-Tropical Megacity in Southern China, as an Example. Atmosphere, 13(9). https://doi.org/10.3390/atmos13091395.
29. Zhou, J. K. , Zhou, Y. K.,&Bai, X. (2023). Can Green-Technology Innovation Reduce Atmospheric Environmental Pollution? Tocics, 11(5). https://doi.org/10.3390/toxics11050403.
30. Chokhachian, A., Perini, K., Giulini, S.,&Auer, T.(2020). Urban permorphologyance and density: Generative study on interdependencies of urban morphology and environmental measures. Sustainable Cities and Society, 53. https://doi.org/10.1016/j.scs.2019.101952.
31. Clark, L.P., Millet, D. B.,&Marshall, J.D. (2011). Air quality and urban morphology in US urban areas: evidence from regulatory monitors. Environmental Science&Technology, 45(16), 7028-7035.
32. Ishii, S., Tabushi, S., Aramaki, T.,et al.(2010). Impact of future urban morphology on the potential to reduce greenhouse gas emissions from residential, commercial and public buildings in Utsunomiya, Japan. Energy Policy, 38(9), 4888-4896.

doi:10.20944/preprints202604.0445.v1

33. Long, Y., Mao, Q.Z., Yang,D.F,&Wang, J.W.(2011). A Multi-agent Model for urban morphology, Transportation Energy Consumption and Environmental Impact Integrated Simulation. Acta Geographica Sinica, 66(8), 1033-1044.
34. Xiang, Y., Ye, Y., Peng, C.C., Teng, M.J.,&Zhou, Z.X.(2022). Seasonal variations for combined effects of landscape metrics on land surface temperature (LST) and aerosol optical depth (AOD). Ecological Indicators, 138. https://doi.org/10.1016/j.ecolind.2022.108810.
35. Zhao, B.B., Tan, X.Y., Luo, L., Deng, M.,&Yang, X.X.(2023). Identifying the Production-Living-Ecological Functional Structure of Haikou City by Integrating Empirical Knowledge with Multi-Source Data. Isprs International Journal Of Geo-Ibmorphologyation, 12(7). https://doi.org/10.3390/ijgi12070276.
36. Shen, Y.,&Zhang, X.W. (2024). Blue Sky Protection Campaign: Assessing the Role of Digital Technology in Reducing Air Pollution. Systems, 12(2). https://doi.org/10.3390/systems12020055.
37. Zhang, Y., Li, Q.Z., Wang, H.Y., Du, X.,&Huang, H.P. (2019). Community scale livability evaluation integrating remote sensing, surface observation and geospatial big data. International Journal of Applied Earth Observation and Geoinmorphologyation, 80, 173-186. https://doi.org/10.1016/j.jag.2019.04.018.
38. Wu,Z.H., Tong, Z.Y., WANG M Z, et al.(2023). Assessing the impact of urban morphological parameters on land surface temperature in the heat aggregation areas with spatial heterogeneity: A case study of Nanjing. Building and Environment, 235: 110232. https://doi.org/10.1016/j.buildenv.2023.110232.
39. Shi Y. R., Zhang Y.F. (2022). Urban morphological indicators of urban heat and moisture islands under various sky conditions in a humid subtropical region. Building and Environment. (214), 108906. https://doi.org/10.1016/j.buildenv.2022.108906.
40. Ku, CA, Tsai, HK.(2020). Evaluating the Influence of Urban Morphology on Urban Wind Environment Based on Computational Fluid Dynamics Simulation. Isprs International Journal of Geo-Inmorphologyation. 9(6). https://doi.org/10.3390/ijgi9060399.
41. Pickett, S.T.A., Cadenasso, M.L., Rosi-Marshall, E.J., Belt, K.T., Groffman, P.M.,&Grove, J.M., et al.(2016). Dynamic heterogeneity: a framework to promote ecological integration and hypothesis generation in urban systems. Urban Ecosystems, 20(1), 1-14. https://doi.org/10.1007/s11252-016-0574-9.
42. Dorigon,L.P,&Amorim, M.C.D.T.(2019). Spatial modeling of an urban Brazilian heat island in a tropical continental climate.URBAN CLIMATE, 28. https://doi.org/10.1016/j.uclim.2019.100461.
43. Xiao, R., Liu, Y., Huang, X., Shi, R., Yu, W.X.,&Zhang, T.(2018). Exploring the driving forces of farmland loss under rapid urbanization using binary logistic regression and spatial regression: A case study of Shanghai and Hangzhou Bay. Ecological Indicators, 95, 445-467. https://doi.org/10.1016/j.ecolind.2018.07.057.
44. Chen, X.D., Zhao, R.F.,Shi, P.J., Zhang, L.X., Yue, X.X., Han, Z.Y., Wang, J.F.,&Dou, H.M. (2023). Land Use Optimization Embedding in Ecological Suitability in the Embryonic Urban Agglomeration. Land, 12(6). https://doi.org/10.3390/land12061164.
45. Guo, W., Teng, Y.J., Yan, Y.G., Zhao, C.W., Zhang, W.Q.,&Ji, X.L.(2022). Simulation of Land Use and Carbon Storage Evolution in Multi-Scenario: A Case Study in Beijing-Tianjin-Hebei Urban Agglomeration,China. Sustainability, 14(20). https://doi.org/10.3390/su142013436.
46. Zhang, X.S., Ren, W.,&Peng, H.J.(2022). Urban land use change simulation and spatial responses of ecosystem service value under multiple scenarios: A case study of Wuhan, China. Ecological Indicators, 144. https://doi.org/10.1016/j.ecolind.2022.109526.